Resilient Structures and Sustainable Construction
Edited by Pellicer, E., Adam, J. M., Yepes, V., Singh, A., and Yazdani, S.

ISBN: 978-0-9960437-4-8

TENSILE CHARACTERIZATION OF TEXTILE REINFORCED MORTAR

ADEL YOUNIS[1], USAMA EBEAD[1], and KSHITIJ SHRESTHA[2]

[1]*Dept of Civil and Architectural Engineering, College of Engineering, Qatar University, Doha, Qatar*
[2]*Institute of Industrial Science, University of Tokyo, Tokyo, Japan*

Textile reinforced mortar (TRM) is a composite material consisting of dry fibers embedded in a cementitious matrix, commonly used for strengthening masonry and concrete structures. In general, tensile characterization is required to identify the TRM mechanical properties, which are considered the key parameters needed for the structural design of strengthening systems. This paper presents the results of an experimental study conducted to investigate the tensile properties of TRM. In this effort, a total of 15 TRM coupons of 410 mm in length, 50 mm in width, and 10 mm in thickness were tested under uniaxial tensile load with clevis-type anchors. Three different types of textile materials were considered: carbon, glass, and polyparaphenylene benzobisoxazole (PBO). As for the study results, a common shape of the TRM tensile constitutive law was observed. Moreover, the average mechanical properties were listed for each type of TRM. Finally, the results and considerations presented in this work can enrich the literature with background data, which are beneficial for future applications of TRM systems in structural rehabilitation and repair.

Keywords: Strengthening, Repair, Structures, Material behavior, Experimentation, Mechanical properties, Test procedure.

1 INTRODUCTION

Structural damages due to deterioration, fatigue, corrosion, creep and shrinkage are commonly encountered in reinforced concrete (RC) structures especially when they are subjected to harsh environmental conditions or unexpected extra loads (Ebead 2015, Ebead *et al.* 2016b, Elghazy *et al.* 2016). Therefore, efficient techniques for strengthening and retrofitting of RC structural members are needed to enhance their loading capacity. Recently, textile reinforced mortar (TRM) has emerged as an excellent alternative to classical strengthening techniques such as externally bonded fiber reinforced polymer, which has been presented in several previous research contributions (Baky *et al.* 2007, Ebead 2011, Ebead and Marzouk 2004, Elsayed *et al.* 2009, Kotynia *et al.* 2008). Textile reinforced mortar is a composite material consisted of dry fibers cemented with an inorganic matrix, generally used for strengthening of masonry and concrete structures (Awani *et al.* 2017, Pino *et al.* 2016).

The TRM tensile mechanical properties are important parameters in the process of the structural design of the TRM strengthening systems (ACI Committee 549 2013). These parameters also form an important basis for effective numerical modeling applications. For that

purpose, a significant research effort has been dedicated in the last few years (Arboleda *et al.* 2016, Carozzi and Poggi 2015, Contamine *et al.* 2011, Ebead *et al.* 2016a) for determination of mechanical characteristics of TRM systems through tensile characterization tests.

The work presented in this paper aims at enriching the literature with further background data pertinent to TRM tensile properties that can be beneficial for future applications of the TRM systems in structural rehabilitation and repair. To achieve this, the axial tensile test has been performed on three different types of commercially available TRM systems. At the outset, the experimental program will be explained including the description of materials, test specimens, test setup, and instrumentation. After that, the experimental results will be presented and discussed, mainly for the stress-strain diagrams and tensile characteristics of the tested specimens.

2 EXPERIMENTAL PROGRAM

2.1 Materials

Three commercially-available TRM systems were implemented in this study, which are: Carbon-TRM (S&P 2016), polyparaphenylene benzobisoxazole (PBO)-TRM (Ruredil 2016), and Glass-TRM (SIKA 2016). Each system consisted of its textile accompanied by the corresponding mortar. The mortar mixtures were prepared as per the manufacturers' recommendations as followed: (a) 4 L of water per 25 kg of mortar for the Carbon-TRM and Glass-TRM systems; and (b) 6.5 L of water per 25 kg of mortar for the PBO-TRM system. The average 28-day compressive strength values provided by the manufacturers for the strengthening mortars are 30 MPa for the PBO-TRM, 40 MPa for the Carbon-TRM, and 58.6 MPa for the Glass-TRM. Table 1 presents the mechanical and geometric properties of each textile type, provided by the manufacturers.

Table 1. Mechanical and geometric properties of the textile in the warp direction.

Textile material	**Center-to-center spacing between strands (mm)**	**Area per unit width, A_f (mm^2/mm)**	**Elastic modulus (GPa)**	**Tensile strength (GPa)**	**Ultimate strain (%)**
Carbon	12	0.157	240	4.30	1.75
PBO	5	0.045	270	5.80	2.15
Glass	14	0.047	80	2.6	3.25

2.2 Test Specimens

TRM specimens were prepared and tested for the tensile characterization as per the AC434 (International Code Council 2013) provisions. First, a 410-mm long, 250-mm wide, and 10-mm thick panel was cast on a flat wooden mold for each type of TRM system. Next, panels were left for a 28-day curing period. After that, each panel was divided to make five test coupons, of dimensions (410 mm x 50 mm x 10 mm). It should be noted that all test coupons contain a single continuous textile layer, associated with the TRM type, of which the warp direction was aligned with the coupon's length.

2.3 Test Setup and Instrumentation

The test setup for the TRM tensile test is shown in Figure 1. A uniaxial tensile load was monotonically applied, in a displacement-controlled routine, at a loading rate of 0.25 mm/s.

Regarding the gripping mechanism, a double clevis-type was applied on the top end, while a single clevis-type connection was applied to the bottom end of the specimen as shown in Figure 1. Metal plates, of 3 mm in thickness, were attached to the ends of the test specimen using epoxy with 150 mm bonding length. Additionally, the extension of the test specimen was measured at each load step by two clip-type displacement transducers fixed on the metal plates as illustrated in Figure 1.

The axial tensile stress (σ_f, in MPa), at any load step, was calculated as the recorded load (P, in N) divided by the TRM equivalent area. This TRM equivalent area was actually considered as the mean textile area per unit width (A_f, in mm^2/m), which is provided for each textile type in Table 1, multiplied by the specimen's width ($w = 50\ mm$), as shown in Eq. (1):

$$\sigma_f(MPa) = \frac{P\ (N)}{A_f\left(mm^2/_{mm}\right) * w(mm)} \tag{1}$$

The corresponding strain in the TRM coupon (ε_{TRM}, in mm/mm) was determined by means of dividing the measured extension of the specimen by the unbonded length (110 mm).

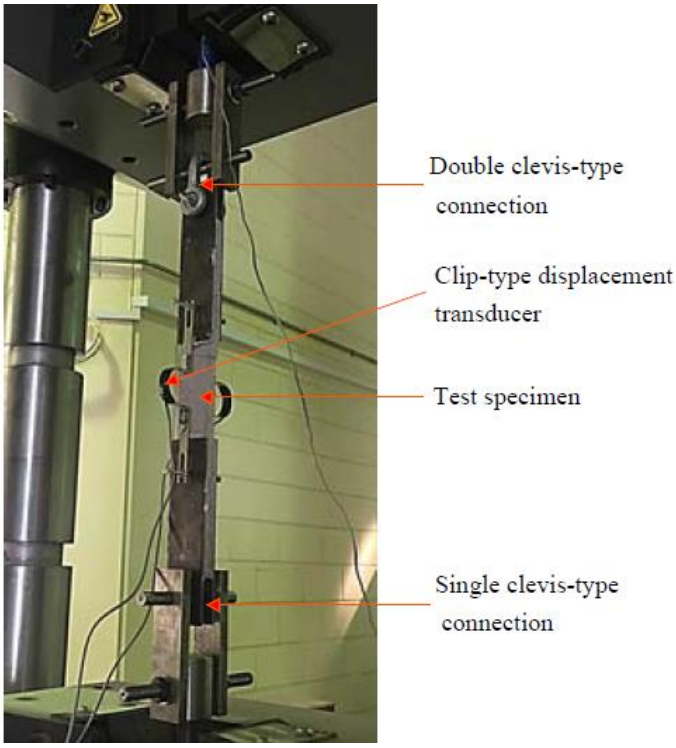

Figure 1. Test setup and instrumentation for the TRM tensile characterization test.

3 RESULTS AND DISCUSSION

The stress-strain diagrams from the uniaxial tensile test performed for each TRM type, Carbon-TRM, PBO-TRM, and Glass-TRM are presented in Figure 2 (a-c). Each diagram is depicted for a representative test specimen of each TRM type. A typical behavior of the TRM tensile constitutive law can be observed for all coupons through the stress-strain relationships shown in Figs 2(a) through (c). In general, two characteristic phases were observed in stress-strain

diagrams: (a) an initial steep curve representing the non-cracked section phase, then (b) a reduced-slope curve corresponded to the cracked section phase.

Unlike the carbon and glass counterparts, the PBO-TRM specimens exhibited a less-brittle type of failure, with no steep drop in the stress-strain diagram at the ultimate stress. About the cracking behavior, it should be noted that all of the cracks have initiated then propagated within the unbonded region of the tested specimens, with no sign of debonding or slippage within the epoxy-bonded zones. In addition, the PBO-TRM coupons exhibited a higher number of cracks than the glass and carbon counterparts.

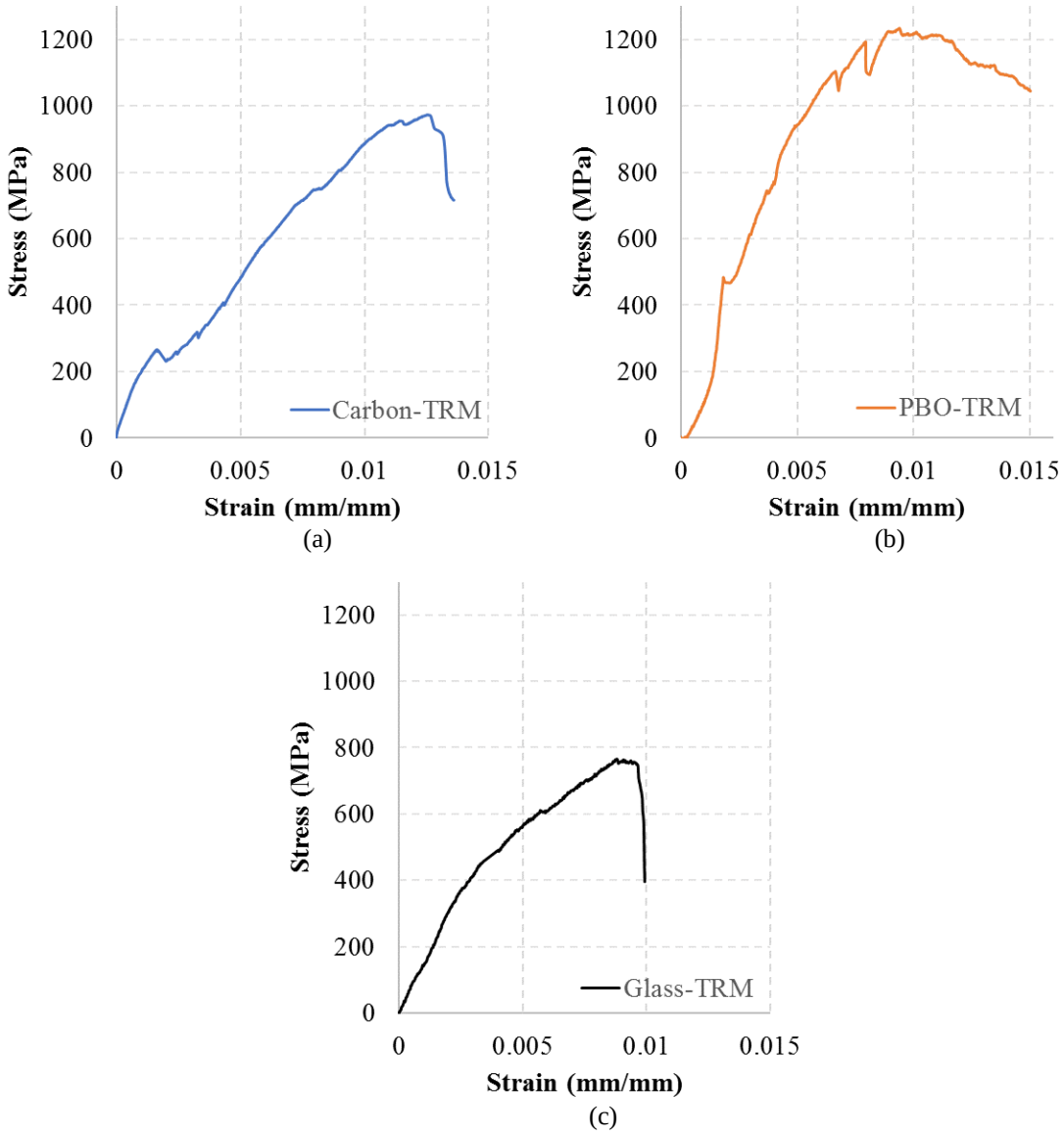

Figure 2. Stress-strain curves for the (a) Carbon-TRM, (b) PBO-TRM, and (c) Glass-TRM tensile coupons.

Table 2 presents the average mechanical properties measured for the tested coupons of Carbon-TRM, PBO-TRM, and Glass-TRM. The first column lists the type of TRM composite,

while the second and third columns of the table list the ultimate tensile stress (σ_{fu}) and ultimate strain (ε_{fu}), respectively. The cracked tensile modulus of elasticity was also determined, as per the AC434 (International Code Council 2013) provisions, for each TRM type and listed in the fourth column of Table 2. Two data points were picked from the cracked response curve to form a segment with stress levels of $\sigma_1 = 0.6\,\sigma_{fu}$ and $\sigma_2 = 0.9\,\sigma_{fu}$, along with their corresponding strain values. The cracked tensile modulus of elasticity (E_f) of TRM can be represented by the slope of the line connecting these two data points, as shown in Eq. (2):

$$E_f(GPa) = \frac{\sigma_2 - \sigma_1}{\varepsilon_{TRM\ at\ \sigma_2} - \varepsilon_{TRM\ at\ \sigma_1}} \tag{2}$$

Table 2. TRM composite tensile characterization properties.

TRM type	σ_{fu} (MPa)	ε_{fu} (%)	E_f (GPa)
Carbon–TRM	975	1.25	74.6
PBO–TRM	1235	1.15	112.3
Glass-TRM	767	1.10	59.7

4 CONCLUSION

An experimental study was performed to measure the tensile properties for three different types of commercially available TRM systems, namely: Carbon-TRM, PBO-TRM, and Glass-TRM. A total number of 15 TRM coupons (410-mm long, 50-mm wide, and 10-mm thick) were tested under uniaxial tensile load with clevis-type anchors. The results of this study revealed a typical pattern of the stress-strain diagrams for the TRM tested coupons representing two distinct phases. The first phase is a steep curve representing the non-cracked section, while the second phase is represented by a gentle curve signifying the cracked section. The average tensile stress and strain values at failure were reported for each TRM composite type. The cracked modulus of elasticities calculated for Carbon-TRM, PBO-TRM, and Glass-TRM were 74.4 GPa, 112.3 GPa, and 59.7 GPa, respectively. To conclude, the results presented in this paper enrich the literature with contextual data, which can be helpful for future applications of TRM composites in strengthening reinforced concrete and masonry structures.

Acknowledgments

This paper was made possible by NPRP grant # NPRP 7-1720-2-641 from the Qatar National Research Fund (a member of Qatar Foundation). The findings achieved herein are solely the responsibility of the authors.

References

ACI Committee 549, *Guide to Design and Construction of Externally Bonded Fabric-reinforced Cementitious Matrix (FRCM) Systems for Repair and Strengthening Concrete and Masonry Structures (ACI 549.4R-13)*, American Concrete Institute, Farmington Hills, MI, USA, 2013.

Arboleda, D., Carozzi, F. G., Nanni, A., and Poggi, C., Testing Procedures for the Uniaxial Tensile Characterization of Fabric-reinforced Cementitious Matrix Composites, *Journal of Composites for Construction*, 20(3), 2016.

Awani, O., El-Maaddawy, T., and Ismail, N., Fabric-reinforced Cementitious Matrix: A Promising

Strengthening Technique for Concrete Structures, *Construction and Building Materials*, Elsevier, 132, 94–111, 2017.

Baky, H. A., Ebead, U. A., and Neale, K. W., Flexural and Interfacial Behavior of FRP-strengthened Reinforced Concrete Beams, *Journal of Composites for Construction*, American Society of Civil Engineers, 11(6), 629–639, 2007.

Carozzi, F. G., and Poggi, C., Mechanical Properties and Debonding Strength of Fabric Reinforced Cementitious Matrix (FRCM) Systems for Masonry Strengthening, *Composites Part B: Engineering*, Elsevier Ltd, 70, 215–230, 2015.

Contamine, R., Si Larbi, A., and Hamelin, P., Contribution to Direct Tensile Testing of Textile Reinforced Concrete (TRC) Composites, *Materials Science and Engineering: A*, 528(29–30), 8589–8598, 2011.

Ebead, U., Hybrid Externally Bonded/Mechanically Fastened Fiber-reinforced Polymer for RC Beam Strengthening, *ACI Structural Journal*, American Concrete Institute, 108(6), 669, 2011.

Ebead, U., Inexpensive Strengthening Technique for Partially Loaded Reinforced Concrete Beams: Experimental Study, *Journal of Materials in Civil Engineering*, American Society of Civil Engineers, 27(10), 4015002, 2015.

Ebead, U. A., Shrestha, K. C., Afzal, M. S., Refai, A. E., and Nanni, A., Effectiveness of FRCM System in Strengthening Reinforced Concrete Beams, *Proceedings of the 4th International Conference in Sustainable Construction Materials and Technologies (SCMT4), University of Nevada, Las Vegas*, 2016a.

Ebead, U., and Marzouk, H., Fiber-reinforced Polymer Strengthening of Two-way Slabs, *ACI Structural Journal*, 101(5), 650–659, 2004.

Ebead, U., Shrestha, K. C., Afzal, M. S., El Refai, A., and Nanni, A., Effectiveness of Fabric-reinforced Cementitious Matrix in Strengthening Reinforced Concrete Beams, *Journal of Composites for Construction*, American Society of Civil Engineers, 4016084, 2016b.

Elghazy, M., Refai, A. E., Ebead, U. A., and Nanni, A., Performance of Corrosion-aged Reinforced Concrete (RC) Beams Rehabilitated with Fabric-reinforced Cementitious Matrix (FRCM), *Proceedings of the 4th International Conference in Sustainable Construction Materials and Technologies (SCMT4), University of Nevada, Las Vegas*, 2016.

Elsayed, W. E., Ebead, U. A., and Neale, K. W., Mechanically Fastened FRP-strengthened Two-way Concrete Slabs With and Without Cutouts, *Journal of Composites for Construction*, American Society of Civil Engineers, 13(3), 198–207, 2009.

International Code Council, *Acceptance Criteria for Masonry and Concrete Strengthening Using Fabric-reinforced Cementitious Matrix (FRCM) Composite Systems (AC434)*, Washington, DC, 2013.

Kotynia, R., Abdel Baky, H., Neale, K. W., and Ebead, U. A., Flexural Strengthening of RC beams with Externally Bonded CFRP systems: Test Results and 3D Nonlinear FE Analysis, *Journal of Composites for Construction*, American Society of Civil Engineers, 12(2), 190–201, 2008.

Pino, V., Hadad, H. A., De Caso, F., Nanni, A., Ebead, U. A., and El Refai, A., *Performance of FRCM Strengthened RC Beams Subject to Fatigue*, 2016.

Ruredil, *Technical datasheet, Ruredil X mesh gold data sheet*, 2016.

S&P, *Technical datasheet, S&P ARMO-mesh technical data sheet*, 2016.

SIKA, *Technical datasheet, SikaWrap-350G Grid data sheet*, 2016.